

SLED: A METHOD OF DOUBLING SLAC'S ENERGY*

Z. D. Farkas, H. A. Hogg, G. A. Loew and P. B. Wilson

Stanford Linear Accelerator Center
Stanford University, Stanford, California 94305

Introduction

Over the past few years, several schemes for making significant increases in the energy of the SLAC beam have been proposed. Two of the proposals, namely the use of superconducting accelerating sections¹ and recirculation of the beam for a second pass through the existing accelerator,² have been abandoned for technical and economic reasons after extensive investigation. An on-going method of gradually raising the beam energy is the development and installation of 30- and 40-MW klystrons by the SLAC Klystron Group. It is clear, however, that the accelerator would have to be completely refitted with klystrons producing about 100 MW in order that the present machine energy be approximately doubled. While such an approach is not inconceivable,³ the realization of such klystrons and the modulators needed to drive them would require further years of development and a high initial capital investment.

Since the accelerator energy is determined by the peak RF input power, and since many experiments are not now limited by average beam power, it was felt that some method for enhancing peak RF power at the expense of RF pulse width might be the answer for increasing SLAC's energy without at the same time increasing the average input power consumption. Standard pulse compression schemes were considered and rejected. One approach that seemed to hold promise, however, came as a result of our experience at SLAC with superconducting cavities. In the course of making measurements on superconducting cavities, it is a common observation that the power radiated from a cavity that is heavily overcoupled approaches four times the incident generator power immediately after the generator has been switched off. Normally this radiated power travels as a reverse wave back toward the generator. There are, however, several microwave networks which can direct this radiated power into an external load; for instance, two identical cavities attached to a 3-dB coupler, as shown in Fig. 1. Using overcoupled cavities, we have in principle a

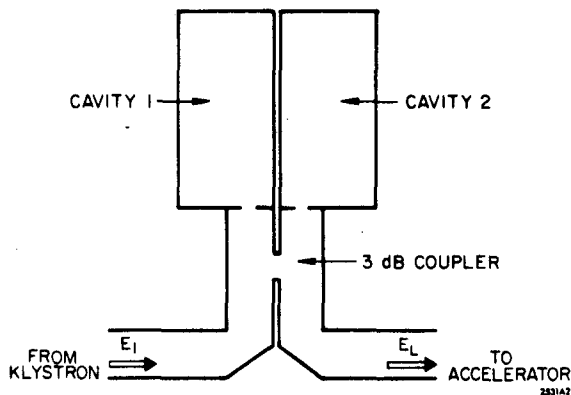


FIG. 1--Schematic drawing of the SLED microwave network.

power multiplier which can enhance peak power by up to a factor of four. This is accomplished, of course, at the expense of pulse width, since the radiated power decays away with a time constant given by the cavity filling time. A further development which enhances the viability of the SLED concept is the observation that if the RF source is reversed in phase rather than simply being switched off, the peak

*Work supported by the U. S. Atomic Energy Commission.

power can be increased by up to a factor of nine. How this comes about is described qualitatively in the following section.

Qualitative Description of SLED

In the case of the present SLAC accelerator, klystrons provide a 2.5 μ sec RF output pulse which travels through a waveguide directly into the accelerating sections as indicated schematically at the top of Fig. 2. In the case of SLED, the

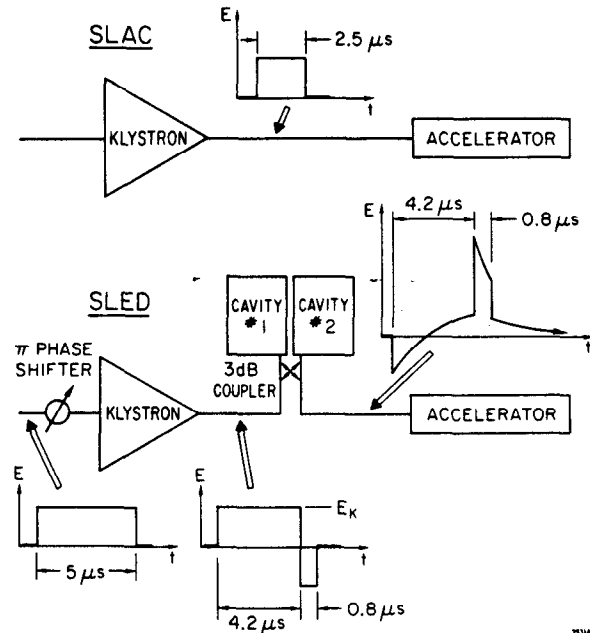


FIG. 2--A comparison of the present SLAC and SLED RF systems.

high-power waveguide system is broken near the klystron and the power divider/dual-cavity assembly shown schematically in Fig. 1 is inserted. The cavities are assumed to be identical and tuned to resonance. After the RF pulse is turned on, the fields in the cavities build up and a wave of increasing amplitude is radiated from the coupling apertures of each cavity. The two emitted waves combine so as to add at the accelerator port of the 3-dB coupler, while they cancel at the klystron port. In addition to the wave emitted from the cavities, a wave travels directly from the klystron to the accelerator. This direct wave, which is just the wave that would appear at the accelerator if both cavities were detuned, is opposite in phase to the combined emitted waves. If the cavities are overcoupled, the emitted wave grows in time to an amplitude which is larger than the direct wave. The net field at the input to the accelerator, which is the sum of the direct and emitted waves, then goes through a phase reversal as shown at the right-center of Fig. 2. One accelerator filling time (0.8 μ sec) before the end of the RF pulse, the π phase shifter reverses the phase of the output wave from the klystron as shown by the waveform at the bottom of Fig. 2. Immediately after this phase reversal, the emitted and direct waves add in phase at the accelerator, since the emitted wave (which is proportional to the stored fields in the cavities) cannot change instantaneously. Therefore, when the klystron phase is reversed, the field at the input to the accelerator increases by two units (assigning one unit to the

direct wave, E_K), since at any instant the load wave is the sum of the direct and emitted waves. Following the phase reversal, the fields in the cavities (and hence the emitted wave also) decrease rapidly as the cavities try to charge up to a new field level of opposite phase. The resultant wave at the accelerator decreases also, as is shown qualitatively in Fig. 2. At the end of the RF pulse, the direct wave goes to zero and the emitted wave only is present at the accelerator. It then decays to zero with a time constant given by the cavity filling time.

Theory

In order to understand the theory of SLED in detail, it is helpful to consider the transient behavior of the reflected and stored fields for a single resonant cavity. As discussed previously, the field which would normally be reflected back toward the generator in the case of a single resonant cavity is directed into the load by means of the microwave network shown in Fig. 2. In analyzing the behavior of a single cavity, it is convenient to consider the net reflected field as the superposition of a wave E_e emitted from the coupling aperture, and a reverse wave E_K which is equal in magnitude to the incident wave E_i from the generator (klystron), and which is reflected from the waveguide-cavity interface with a 180° -phase reversal. If at any instant the generator is turned off, the field traveling away from the cavity is equal to E_e , which in turn is proportional to the stored field inside the cavity at that time. If, on the other hand, at any instant the cavity could be emptied of stored energy (by, for example, instantaneously detuning it) then the reverse wave traveling back toward the generator would be just E_K . By conservation of power,

$$P_K = P_L + P_c + dW_c/dt,$$

where P_K is the incident power, P_L is the net reflected power (the power delivered to the load in the case of the SLED network shown in Fig. 2), P_c is the power dissipated in the cavity and W_c is the energy stored in the cavity at time t . Using $P_c = \omega W_c/Q_0$, together with the fact that power is proportional to the square of the field, ($P = kE^2$), the above relation becomes

$$E_K^2 = (E_e + E_K)^2 + E_e^2/\beta + (2Q_0/\omega\beta)E_e dE_e/dt.$$

A cavity coupling coefficient β has also been defined, such that $kE_e^2 = \beta P_c$. If at any instant the generator is turned off, β is given by the ratio of the power emitted from the coupling aperture to the power dissipated in the cavity walls. If we now introduce the cavity filling time $T_c = 2Q_0/\omega = 2Q_0/[\omega(1+\beta)]$, the preceding expression can be rearranged to give

$$T_c dE_e/dt + E_e = -\alpha E_K, \quad (1)$$

where $\alpha = 2\beta/(1+\beta)$.

Equation (1) can now be solved for the generator waveform E_K shown at the top of Fig. 3. For convenience, we take E_e to be initially positive, and since initially E_e and E_K must be opposite in phase, we take E_K to be -1 . At time t_1 the phase of the generator wave is reversed, and $E_K = +1$. At time t_2 the incident power is turned off. By solving Eq. (1), the following expressions for the emitted field in the three time intervals A, B and C shown in Fig. 3 are obtained:

$$E_e(A) = -\alpha e^{-T} + \alpha; \quad E_{e1} = -\alpha e^{-T_1} + \alpha; \quad (2a)$$

$$E_e(B) = \gamma e^{-(T-T_1)} - \alpha; \quad E_{e2} = \gamma e^{-(T_2-T_1)} - \alpha; \quad (2b)$$

$$E_e(C) = E_{e2} e^{-(T-T_2)} \quad (2c)$$

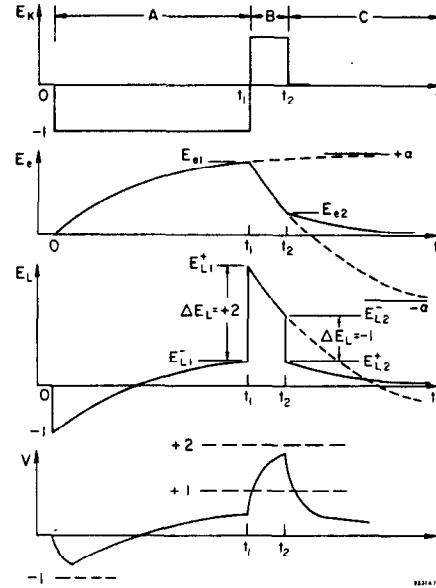


FIG. 3--Direct wave E_K , emitted wave E_e , and net load wave E_L for SLED.

where $\tau \equiv t/T_c$, $\gamma \equiv \alpha(2 - e^{-T_1})$ and E_{e1} and E_{e2} are the values of E_e at t_1 and t_2 . The variation in E_e as a function of time is shown in Fig. 3 for the case $\beta=5$, $\tau_1=2$ and $\tau_2=2.4$. The load waveform, given by $E_L = E_K + E_e$, is also shown in Fig. 3. The load fields are:

$$E_L(A) = E_e(A) - 1 = -\alpha e^{-T} + (\alpha - 1) \quad (3a)$$

$$E_L(B) = E_e(B) + 1 = \gamma e^{-(T-T_1)} - (\alpha - 1) \quad (3b)$$

$$E_L(C) = E_e(C) = [\gamma e^{-(T_2-T_1)} - \alpha] e^{-(T-T_2)} \quad (3c)$$

The field on a traveling-wave constant-gradient accelerating section is given by $E(z, t) = E[0, t - \Delta t(z)]$, where $\Delta t(z)$ is the length of time it takes for a wave to propagate from the input of the structure to position z on the structure. For a constant-gradient structure, in which the group velocity varies linearly with z according to $v_g(z) = v_{g0}(1 - gz/L)$, the propagation time to position z is given by

$$\Delta t(z) = \int_0^z \frac{dz}{v_g(z)} = \int_0^z \frac{dz}{v_{g0}(1 - gz/L)}.$$

Defining $z' = z/L$, where L is the length of the accelerating structure, and integrating the above expression, we obtain

$$\Delta t(z') = T_a [\ln(1 - gz')/\ln(1 - g)] \quad (4)$$

where $T_a = \Delta t(1) = (L/gv_{g0}) \ln[1/(1 - g)]$ is the filling time for the structure. The field $E(z, t)$ along the structure is now obtained by substituting $t - T_a [\ln(1 - gz')/\ln(1 - g)]$ for t in Eqs. (3). The result is:

$$E(A) = -\alpha e^{-T} f(z') + (\alpha - 1) \quad (5a)$$

$$E(B) = \gamma e^{-(T-T_1)} f(z') - (\alpha - 1) \quad (5b)$$

$$E(C) = [\gamma e^{-(T_2-T_1)} - \alpha] e^{-(T-T_2)} f(z') \quad (5c)$$

where $f(z') = (1 - gz')^\nu$ and $\nu = (T_a/T_c) [\ln(1 - g)]^{-1}$.

In using these relations, the fact must be taken into account that there are discontinuities in the field along the accelerating structure corresponding to discontinuities at

times $t_d=0$, t_1 and t_2 in the field as a function of time at the input to the structure. In general, a field discontinuity will occur at a position z'_d along the structure for a discontinuity at time t_d in the waveform at $z=0$, where

$$z'_d = (1/g) \left[1 - (1-g)^{(t'-t'_d)} \right] \quad (6)$$

This expression is obtained by solving Eq. (4) for z' , defining also a normalized time by $t' = t/T_a$, and setting $\Delta t = t - t_d$. For example, in the time interval $0 < t < t_1$, the field is zero for $z' > z'_d$, where z'_d is obtained using $t'_d = 0$ in Eq. (6). For $z' < z'_d$, the field is given by Eq. (5a).

The accelerating voltage is now obtained by integrating the field from $z' = 0$ to $z' = 1$, taking into account the location of the field discontinuities and using the appropriate fields given by Eqs. (5) up to and following each discontinuity. Thus the energy gain V for the interval $t_1 < t < t_2$ is given by

$$V = \int_0^{z'_{d1}} E(B) dz' + \int_{z'_{d1}}^1 E(A) dz' ,$$

where z'_{d1} is given by Eq. (6) with $t'_d = t'_1$. The energy gain is by definition unity after one filling time for a direct wave $E_K = 1$, which would be present with the cavities detuned. Since $f(z')$ is common to all of the energy gain integrals, the calculation is simplified by defining

$$F_1(z'_d) = \int_0^{z'_d} f(z') dz' = \left[1 - (1-gz'_d)^{1+\nu} \right] [g(1+\nu)]^{-1} ;$$

$$F_2(z'_d) = \int_{z'_d}^1 f(z') dz' = \left[(1-gz'_d)^{1+\nu} - (1-g)^{1+\nu} \right] [g(1+\nu)]^{-1} .$$

Thus, during $t_1 < t < t_2$,

$$V = \gamma e^{-(T-\tau_1)} F_1(z'_d) - (\alpha-1) z'_{d1} - \alpha e^{-\tau} F_2(z'_d) + (\alpha-1)(1-z'_{d1})$$

Similar expressions can be derived for time intervals A and C. A plot of the normalized energy gain as a function of time is given at the bottom of Fig. 3. The maximum energy is obtained after one filling time, by letting $t = t_1 + T_a$ (or $t' = t'_1 + 1$) and $z'_{d1} = 1$. For this special case,

$$V_{\max} = M = \gamma e^{-T_a/T_c} \left[1 - (1-g)^{1+\nu} \right] [g(1+\nu)]^{-1} - (\alpha-1) \quad (7)$$

Further details of the SLED theory are given by Farkas⁴ and Wilson.⁵ The effect of cascading several of the microwave networks shown in Fig. 1 was calculated⁴ in the hope of obtaining flatter output pulses and perhaps still higher values for the energy multiplication factor. Somewhat flatter output pulses were predicted, but not higher multiplication factors in the examples investigated. The possibility cannot be ruled out, however, that other more favorable configurations might be found.

Choice of Parameters

An analysis of Eq. (7) shows that the maximum energy gain M approaches 3 if $\beta \gg 1$, $T_c \gg T_a$ and $t_1 \gg T_c$. Since $T_c(1+\beta) = 2Q_0/\omega$, it is impossible to have both a large filling time and a large coupling coefficient unless the

unloaded Q of the cavities can be made arbitrarily large. However, the unloaded Q of a practical room-temperature resonator is limited to about 10^5 . The RF pulse length is also limited by practical considerations. The present pulse length, t_2 , of SLAC is 2.5 μ sec. It is reasonable to consider doubling this pulse length to 5.0 μ sec. Figure 4 shows the

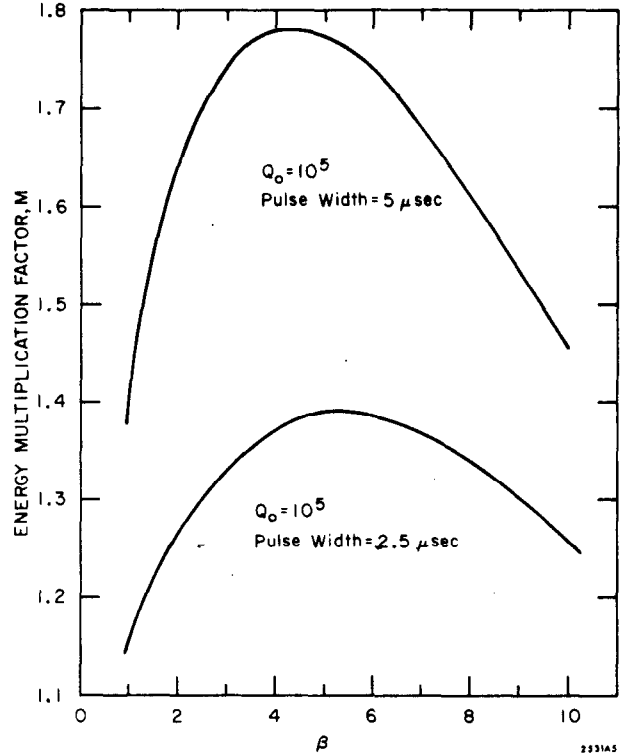


FIG. 4--Energy multiplication factor as a function of cavity coupling coefficient.

energy multiplication factor as a function of the cavity coupling coefficient for these two pulse lengths with $Q_0 = 10^5$. It is seen that the energy gain is maximum for a coupling coefficient in the range $\beta = 4$ to 5. Figure 5 shows the energy multiplication factor M as a function of unloaded Q for various values of RF pulse length, and Fig. 6 gives M as a function of pulse length for various values of Q_0 . The coupling coefficient has been optimized at each point on the curves in both figures to give the maximum energy gain. It is seen that the longer the pulse length and the higher the unloaded Q , the greater is the energy gain.

As a result of a number of practical and economic considerations, the parameters proposed for SLED are $Q_0 = 10^5$, $t_2 = 5.0 \mu$ sec and $\beta \approx 4.5$. The energy multiplication factor for these values is 1.78. Figure 7 shows the RF power output from the SLED microwave network as a function of time for these parameters. The "pulse compression" effect of the SLED network is clearly seen.

Beam Loading

Figure 8 shows the unloaded relative energy gain as a function of time in the region of peak energy for the SLED parameters as chosen in the previous section. It is clear that the pulse length of a beam accelerated near peak energy will necessarily be short compared to the structure filling time. The unloaded energy is seen to be increasing as a function of time as peak energy is approached. By turning on the beam prior to reaching peak energy, the transient energy droop due to beam loading can be used to produce a rough compensation for the rising unloaded energy gain, resulting in a considerably tighter energy spectrum. For SLAC, the transient beam

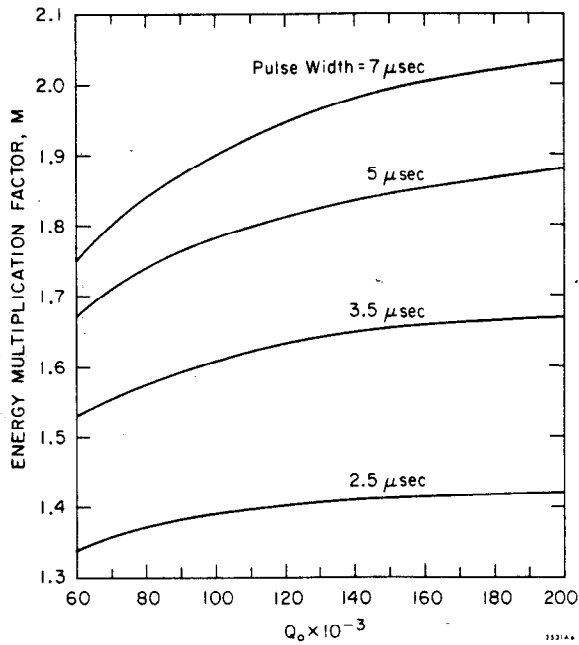


FIG. 5--Energy multiplication factor as a function of unloaded Q .

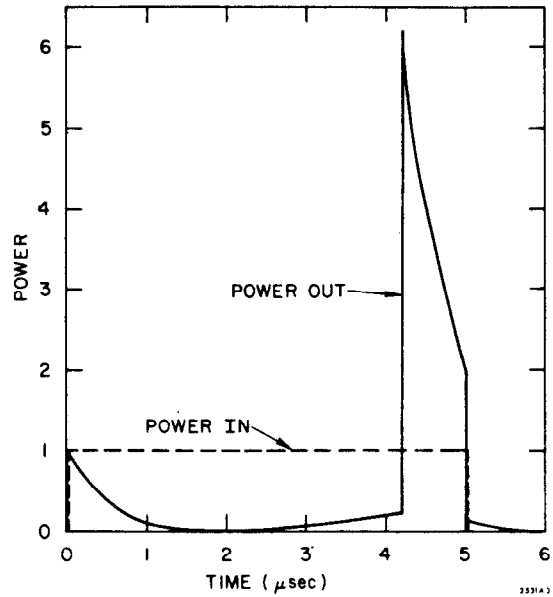


FIG. 7--Input power to and output power from the SLED microwave network as a function of time.

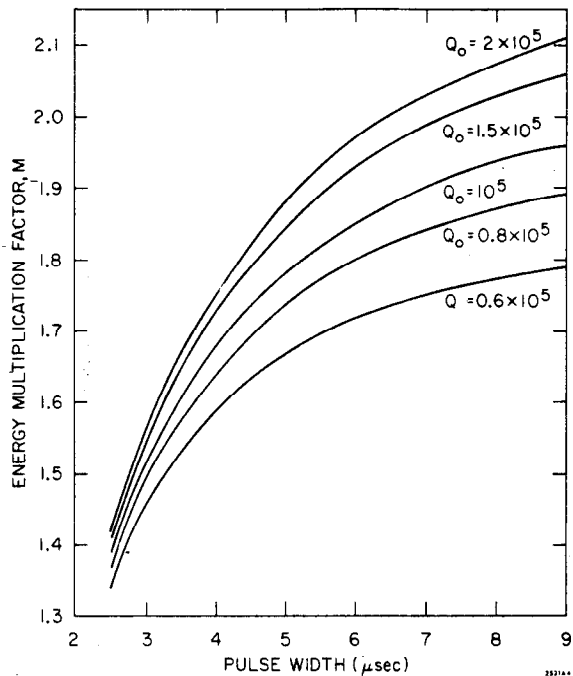


FIG. 6--Energy multiplication factor as a function of pulse width.

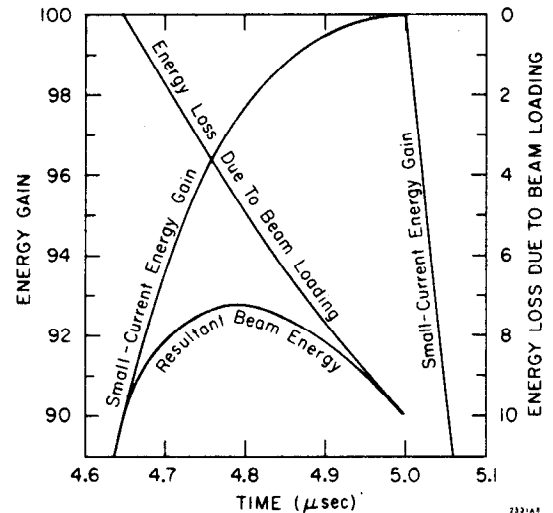


FIG. 8--Unloaded energy gain, energy droop due to beam loading and resultant beam energy for a beam pulse length of 0.35 μsec .

loading voltage is given, to the accuracy required here, by

$$V_b (\text{MV}) = 35 i_p \left[2 \Delta t / T_a - (\Delta t / T_a)^2 \right],$$

where i_p is in milliamperes and Δt is the time after the beam has been switched on. Figure 8 also shows the transient variation in the relative beam loading as a function of time for a maximum unloaded energy of 46 GeV and a peak current of 200 mA, assuming that the beam is switched on 0.35 μsec before the peak energy is reached. The curve of the resultant beam energy shows that beam loading compensation has reduced the variation in energy gain over this time interval from 10% to about 2½%. Table I gives the

loaded energy V , the peak current i_p , the average current i_{ave} and the energy spectrum width $\Delta V/V$ for various values of the beam pulse length T_b . For each value of T_b , the peak current has been chosen so that the beam energy is the same at the beginning and end of the pulse. The maximum unloaded energy is taken as 46 GeV, which would be obtained from the SLAC linac for an energy multiplication factor of 1.78 and a klystron power of 30 MW. A repetition rate of 180 pps has been assumed in computing the average current.

By shaping the current pulse as a function of time, the energy spectrum widths can in principle be reduced considerably below the values given in Table I for a constant pulse current. Likewise, by advancing the triggers to a fraction of the klystrons along the machine, the peak current for a given beam pulse length can be reduced below the values shown in Table I while still maintaining a tight energy spectrum. The peak pulse current for SLED will in practice be limited by beam breakup. For the present SLAC focusing

Table I
SLED Beam Loading Characteristics (30 MW klystrons)

T_b (μsec)	V (GeV)	i_p (mA)	i_{ave} (μA)	$\Delta V/V$ (%)
0	46.0	0	0	0
0.10	45.8	31	0.6	0.15
0.15	45.4	54	1.5	0.4
0.20	44.8	80	2.9	0.7
0.25	44.0	110	4.9	1.1
0.30	43.0	143	7.7	1.7
0.35	41.8	181	11.4	2.4
0.40	40.3	224	16.2	3.3

configuration and beam energy, beam breakup limits the peak current to 160 mA for a beam pulse length of 0.3 μsec . At a final energy of 40 GeV, a pulse current on the order of 250 mA could be accelerated at this pulse length, assuming a reasonable increase in the strength of the focusing along the accelerator.

In Table II, the parameters for the present SLAC accelerator and for SLED are summarized for a beam-loaded

Table II
Comparison of SLED and Present SLAC Parameters

		Present SLAC (30 MW klystrons)	SLED (30 MW klystrons)	SLED (40 MW klystrons)
Unloaded Energy	(GeV)	26	46	53
Loaded Energy	(GeV)	23.5	41.5	46
Repetition Rate	(pps)	360	180	180
RF Pulse Length	(μsec)	2.5	5.0	5.0
Beam Pulse Length	(μsec)	1.6	0.36	0.36
Average Current	(μA)	40	12.5	14.5
Peak Current	(mA)	70	190	220
Electrons per Pulse		7×10^{11}	4.5×10^{11}	5×10^{11}
Duty Cycle		6×10^{-4}	6.5×10^{-5}	6.5×10^{-5}
Energy Spread	(%)	~ 1.0	$< 1.0^*$	$< 1.0^*$
Average Beam Power	(kW)	950	520	700

*Assumes current pulse shaping (e.g., 230 mA for the first half of the pulse, then 160 mA for the second half for the case of 30 MW klystrons). For constant peak current, estimated energy spread is 2.5%.

energy 10% below the unloaded energy. Parameters for SLED are given for both 30 and 40 MW klystrons; at the time SLED becomes operational, the average peak klystron power per station is expected to lie between these limits.

SLED Cavity Design

As noted in the previous sections, cavities with Q_0 on the order of 10^5 are needed to obtain a power multiplication factor high enough to be of interest. This Q_0 can be obtained in copper cavities operating at or somewhat above room temperature if a higher-order resonant mode is employed. Considerations of cost, mechanical stability and frequency separation of competing modes make it desirable to choose the mode with the smallest cavity volume for a specified Q_0 . Modes which are members of the TE_{01n} family have this desirable characteristic. The value $n=5$ was chosen as optimum for our purposes. The ratio of diameter D to length L for the cavity remained to be determined. A value of D/L less than unity (which gives maximum Q_0) was chosen on the basis of material availability.

A smaller diameter also reduces the deformation of the end-plates due to atmospheric pressure loading. The exact ratio (D/L=0.611) was selected to maximize frequency separation from competing modes. The TM_{115} mode, which is normally degenerate with the TE_{015} mode, was lowered approximately 24 MHz by cutting a circular groove at the outer diameter in one end-plate. This groove does not disturb the TE_{015} mode field pattern or frequency. In summary, the selected parameters for the SLED prototype cavity are:

$$\begin{aligned} \text{Diameter} &= 20.51 \text{ cm} \\ \text{Length} &= 33.59 \text{ cm} \\ *Q_0 &= 1.08 \times 10^5 \end{aligned}$$

*Theoretical Q for copper at $f_0 = 2856 \text{ MHz}$

The rate of change of frequency with temperature is $-48 \text{ kHz}/^\circ\text{C}$ for copper construction.

Preliminary analysis has indicated that a cavity tuning error of 10 degrees is acceptable. Assuming $Q_0 = 10^5$ and $\beta=5$, the loaded Q is $Q_L = 1.6 \times 10^4$. Thus the cavity half-bandwidth, $\frac{1}{2} BW$, is approximately 90 kHz. If Δf is the difference between the driving frequency and the cavity resonant frequency, the cavity tuning angle is given by $\psi = \tan^{-1} [\Delta f / (\frac{1}{2} BW)]$. Thus, if ψ is to be limited to ± 10 degrees, Δf must not be greater than 16 kHz. From the tuning rate with temperature given above, this implies that the cavity temperature must be held constant to within $1/3^\circ\text{C}$. The existing accelerator cooling water system holds temperature fluctuations to better than $\pm 0.15^\circ\text{C}$, which would appear to be adequate. However, the RF power dissipated inside each cavity, which is calculated to be about 2 kW average for a 30 MW klystron source, will raise the metal temperature on the order of 1.4°C . This temperature change will shift the resonant frequency by 67 kHz and introduce a tuning error of 37 degrees. Although the cavities may be pre-tuned to 2856 MHz at the equilibrium temperature with the RF power on, there will still be a phase- and amplitude-drift period during warm-up following each RF shutdown. The severity of this problem will be gauged during prototype tests. The concept of a mechanically temperature-compensated cavity has been suggested and will be tried if necessary.

A cross-sectional drawing of the prototype assembly is shown in Fig. 9. The cavity cylinders are made from copper forgings, machined to 9.5 mm wall thickness. The inner surface finish is better than 0.15 microns (RMS). Water-cooling tubes are brazed on in pairs covering the five zones of maximum heat dissipation along each cylinder. The cavities are fine-tuned by distorting the thin-wall end-plate using a differential screw. The tuning range is approximately $\pm 1 \text{ MHz}$. Coupling between the cavity and waveguide magnetic fields is achieved through circular apertures in the end-plates. A 2.77 cm diameter aperture in a 4.06 mm thick wall gives the desired β value for $Q_0 = 10^5$.

It is anticipated that there will be frequent need to run the accelerator in the present non-SLED mode; that is, with the flat-topped RF pulse from the klystron transmitted without distortion to the accelerator. This can be done by detuning the SLED cavities, which then appear as short-circuits across two ports of the 3-dB hybrid coupler. Under these conditions, the klystron pulse is transmitted through the SLED network without significant reflection or loss. The design requirements placed upon the detuner are quite severe. Primarily, when it is moved from the "detuned" to the "tuned" position, it must return the cavity to the same resonant frequency to within a few kilohertz. Also, in the "tuned" position, it must not degrade the cavity Q_0 nor introduce any frequency modulation due to mechanical vibration. A prototype detuner has been designed which consists

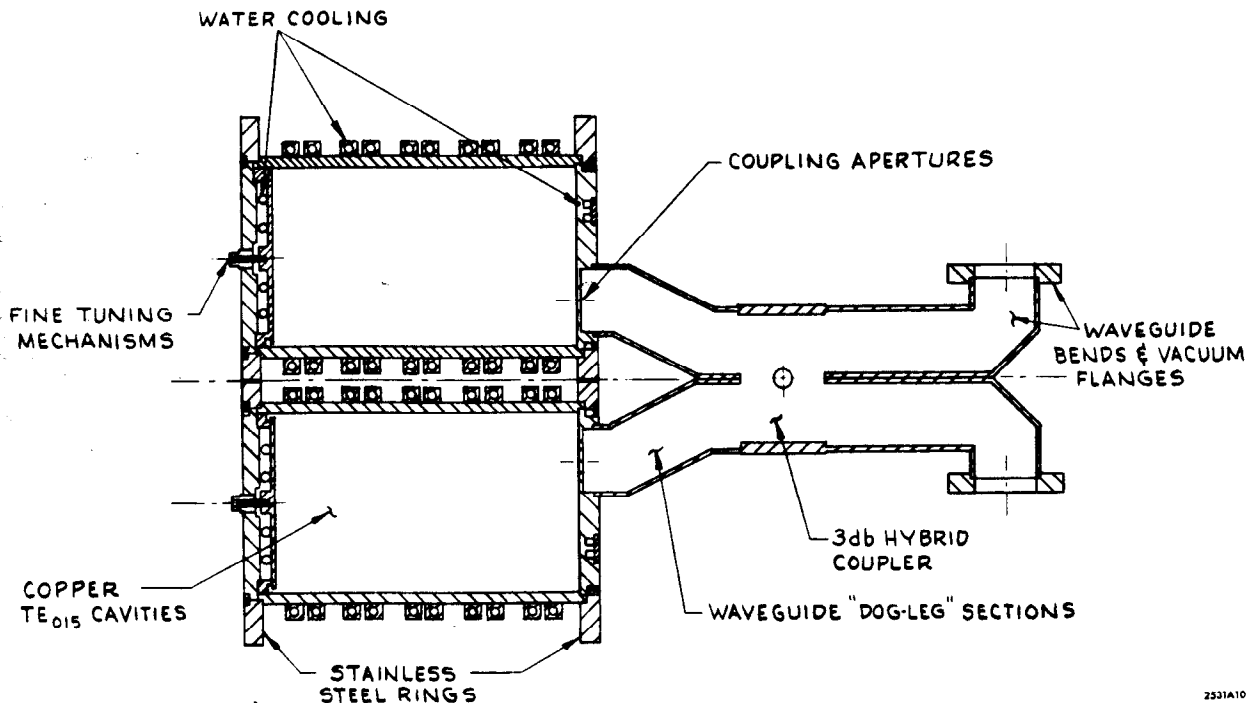


FIG. 9--Assembly drawing of the prototype microwave network for SLED.

of a stainless steel needle 1.52 mm in diameter inserted into the TE_{015} cavity through a 2.03 mm hole in the cavity wall. This hole enters the cavity on a current node and thus causes negligible perturbations of f_0 and Q_0 . The needle enters at an angle such that when fully inserted, its tip reaches a circle of maximum azimuthal E field. In this way a detuning of 18 MHz, or approximately 100 bandwidths, is achieved. In its fully retracted position, the needle is decoupled by at least 90 db from the cavity fields and has no residual effect upon f_0 and Q_0 .

The SLED prototype assembly described above has performed very well in low-power tests at room temperature. The "detuned" and "tuned" output waveforms follow very closely the "Power In" and "Power Out" curves, respectively, shown in Fig. 7. High-power tests into a matched load are presently in progress. In September of this year, the prototype cavity-hybrid unit will be installed as shown in Fig. 10 on a klystron station near the accelerator injector to allow tests to be made with a beam.

If SLED is to be a viable means for increasing the energy of the SLAC linac, it must be shown that the klystrons can operate satisfactorily at the 5.0 μ sec RF pulse length and 180 pps repetition rate required. Initial tests at the longer pulse length indicate that the klystron fault rate is somewhat higher than is the case at the present 2.5 μ sec pulse length, but there is no evidence that the klystrons will not operate satisfactorily under the SLED conditions.

SLED Modes of Operation and Physics Possibilities

Boosting the energy of the present SLAC accelerator into the 40- to 50-GeV range by means of SLED makes available a number of new operating modes for the machine and a corresponding variety of possibilities for the high energy physics program. The full exploitation of the SLED idea requires that all 245 high-power klystron stations be equipped with microwave cavity networks; new pulse-forming networks and pulse transformers must be added to the modulators as well. The combination of these two features gives

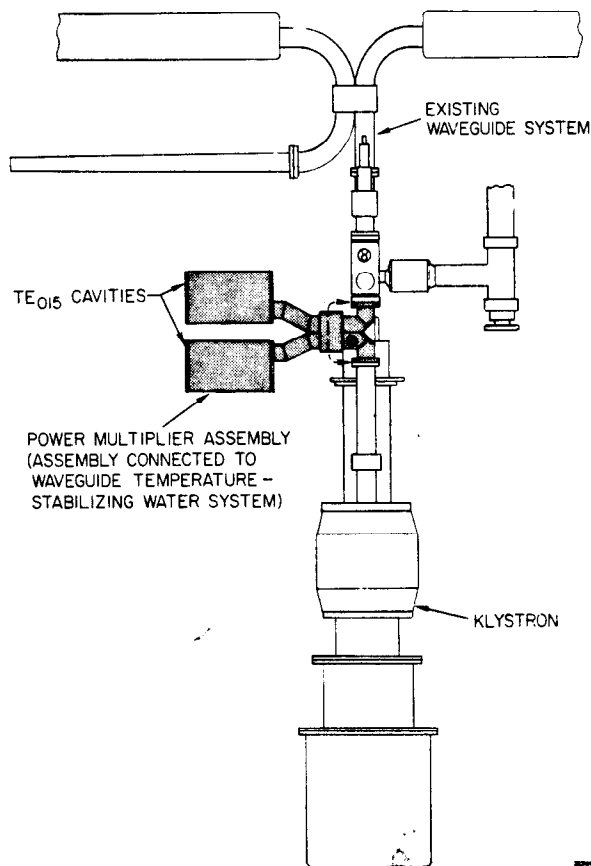


FIG. 10--Proposed installation of the SLED microwave network at a typical station in the Klystron Gallery.

a 5 μ sec RF pulse at the output of each klystron and boosts its effective peak power from 30 to 100 MW. This enhancement in peak power is achieved at the cost of reducing the repetition rate from 360 pps to 180 pps and the beam duty cycle by a factor of 10. The present plan is to make these modifications reversible. The cavity detuners which have been described above can be inserted in a fraction of a second. This results in a possible machine operating mode at the present energy (~ 23 GeV) but with a beam pulse length of 4.2 μ sec, giving an improvement in duty cycle over present operation (at 360 pps) of over 30%. This mode of operation cannot be interlaced on a pulse-to-pulse basis with the SLED high-energy mode, but is obtainable after a short switch-over time. It will be used for phasing the machine, possibly for injection of 1.5 GeV electrons and positrons into SPEAR, and for ~ 20 GeV beams for experiments such as LASS (Large Aperture Solenoidal Spectrometer). An alternate method of obtaining low-energy beams might be to inject electrons on an early part of the energy gain waveform. Early injection will be made possible by not installing SLED cavities on the injector klystrons, thereby having a flat 5 μ sec RF pulse available for capture. When the present mode of operation at 360 pps needs to be restored, this will be done by halving the lengths of the new pulse-forming networks in the modulators. The switch-over might be done by remote control. Even if done manually, the operation should not take more than an hour or so for the entire machine. It is important to point out that none of these modes of operation require an increase in average power for the accelerator above the ~ 25 MW that is presently used.

A full discussion of the physics possibilities opened by SLED is beyond the scope of this report. Only a few general remarks will be made here. It appears that End Station A would continue to be the main experimental center for electron scattering and photoproduction physics. In order to bend the 40- to 50-GeV beams into the A-line, three out of the five 0.1° pulsed magnets at the apex of the beam switchyard (BSY) would be replaced by stronger magnets and power supplies. The eight 3° bending magnets which make up the 24° A-bend would also be replaced by stronger magnets. The A-beam dump magnets used for photon experiments would be upgraded. What modifications would be made in the spectrometers is not yet clear.

The main "ecological" change in the research yard would take place in the mix of experiments between End Stations B (ESB) and C (ESC). For higher-energy RF-separated K^\pm and antiproton beams, there is insufficient drift distance behind ESB in the Research Yard. For this reason, it has been proposed that the RF separators be moved to the present C-beam, which would be rebuilt with the target moved up by about 100 m. This change might eventually cause LASS and/or the bubble chamber to be moved to the C-beam. The K^0 -decay experiments in ESB may not require higher energies than at present (and therefore no modifications), but production experiments with K^0 's may be exploitable. It is also possible that higher-energy primary e^- or photon beams may be of interest to LASS in its present location (or in ESC). In any case, upgrading the 12° B-line would be fairly inexpensive because one would simply add some of the 3° magnets available from the A-line. ESC, on the other hand, would be more drastically modified, but at relatively low cost since no large-angle bends would be involved. The proposed plan would be to create three independent channels by means of a magnetic slit located downstream of the present tune-up dump. The pulsed magnets at the apex of the BSY would aim the electron beam from the accelerator into any one of these three channels. The central beam would be charged (separated beams mentioned above), and the other two would be neutral. One of these neutral beams might consist of photons derived from the collision of electrons with a beam of photons from a laser or from coherent bremsstrahlung; it would be used by the streamer chamber. The other might be a K^0 beam.

The present cost estimates for SLED (at FY 1974 rates, excluding project indirects, design and engineering, and contingency) break down roughly as follows:

Microwave System	\$~1 M
Modulator Modifications	~1.9 M
Instrumentation and Control	~0.5 M
Beam Switchyard Modifications	~1.6 M
Total	\$ 5.0 M

Acknowledgements

The authors acknowledge the work that has been carried out by the SLAC Klystron Group, under J. Lebacqz, to test and evaluate the performance of the SLAC klystrons at the longer pulse length required by SLED. C. Olson and the Accelerator Electronics Group have made design and engineering studies of the modifications required to increase the pulse length of the SLAC modulators, and have carried out those modifications on an initial unit for long pulse klystron tests. A. Lisin and R. Sandkuhle have been responsible for the mechanical design of the SLED prototype assembly. Fabrication and scheduling were directed by H. Zaiss. K. Mallory has studied the instrumentation and control problems associated with SLED, and D. Walz has investigated the changes required to upgrade the beam switchyard. J. Murray and L. Keller with many others have studied the high energy physics possibilities opened up by SLED. H. Deruyter has been responsible for all microwave measurements involved in the development and testing of the cavity-hybrid microwave network.

References

1. P. B. Wilson et al., Particle Accelerators 1, 223 (1970).
2. W. B. Herrmannsfeldt et al., Proc of the 8th Int. Conf. on High Energy Accelerators (CERN-Scientific Information Service, Geneva, 1971), p. 563.
3. G. A. Loew, "Electrons, the Energy Crisis and the Possibilities of RF power," SLAC RLA Note 52, Stanford Linear Accelerator Center, Stanford University, Stanford, California (June 1973), unpublished.
4. Z. D. Farkas, "Power Multiplier," Technical Note SLAC-TN-73-8, Stanford Linear Accelerator Center, Stanford University, Stanford, California (September 1973), unpublished.
5. P. B. Wilson, "SLED: A Method for Doubling SLAC's Energy," Technical Note SLAC-TN-73-15, Stanford Linear Accelerator Center, Stanford University, Stanford, California (December 1973), unpublished.